Shifts in the community structure and activity of anaerobic ammonium oxidation bacteria along an estuarine salinity…

Article *in* Journal of Geophysical Research: Biogeosciences · June 2016

DOI: 10.1002/2015JG003300

CITATION
1

READS
214

10 authors, including:

Yanling Zheng
East China Normal University
28 PUBLICATIONS **234** CITATIONS
SEE PROFILE

Lijun Hou
East China Normal University
98 PUBLICATIONS **1,323** CITATIONS
SEE PROFILE

Juan Gao
East China Normal University
17 PUBLICATIONS **71** CITATIONS
SEE PROFILE

Xiaofei Li
East China Normal University
33 PUBLICATIONS **162** CITATIONS
SEE PROFILE

AGU PUBLICATIONS

JGR

Journal of Geophysical Research: Biogeosciences

RESEARCH ARTICLE
10.1002/2015JG003300

Key Points:
- Significant shift in anammox community structure along the salinity gradient was observed ($P < 0.01$)
- Anammox bacterial abundance was significantly positively correlated with salinity ($P < 0.05$)
- Contribution of anammox to N removal was significantly negatively correlated with salinity ($P < 0.01$)

Supporting Information:
- Supporting Information S1

Correspondence to:
L. Hou and M. Liu,
ljhou@sklec.ecnu.edu.cn;
Mliu@geo.ecnu.edu.cn

Citation:
Zheng, Y., X. Jiang, L. Hou, M. Liu, X. Lin, J. Gao, X. Li, G. Yin, C. Yu, and R. Wang (2016), Shifts in the community structure and activity of anaerobic ammonium oxidation bacteria along an estuarine salinity gradient, *J. Geophys. Res. Biogeosci.*, *121*, doi:10.1002/2015JG003300.

Received 3 DEC 2015
Accepted 23 MAY 2016
Accepted article online 2 JUN 2016

Shifts in the community structure and activity of anaerobic ammonium oxidation bacteria along an estuarine salinity gradient

Yanling Zheng[1,2], Xiaofen Jiang[2], Lijun Hou[2], Min Liu[1], Xianbiao Lin[1], Juan Gao[2], Xiaofei Li[1], Guoyu Yin[1,2], Chendi Yu[2], and Rong Wang[2]

[1]College of Geographical Sciences, East China Normal University, Shanghai, China, [2]State Key Laboratory of Estuarine and Coastal Research, East China Normal University, Shanghai, China

Abstract Anaerobic ammonium oxidation (anammox) is a major microbial pathway for nitrogen (N) removal in estuarine and coastal environments. However, understanding of anammox bacterial dynamics and associations with anammox activity remains scarce along estuarine salinity gradient. In this study, the diversity, abundance, and activity of anammox bacteria, and their potential contributions to total N_2 production in the sediments along the salinity gradient (0.1–33.8) of the Yangtze estuarine and coastal zone, were studied using 16S rRNA gene clone library, quantitative polymerase chain reaction assay, and isotope-tracing technique. Phylogenetic analysis showed a significant change in anammox bacterial community structure along the salinity gradient ($P < 0.01$), with the dominant genus shifting from *Brocadia* in the freshwater region to *Scalindua* in the open ocean. Anammox bacterial abundance ranged from 3.67×10^5 to 8.22×10^7 copies 16S rRNA gene g^{-1} and related significantly with salinity ($P < 0.05$). The anammox activity varied between 0.08 and 6.46 nmol N g^{-1} h^{-1} and related closely with anammox bacterial abundance ($P < 0.01$). Contributions of anammox activity to total N loss were highly variable along the salinity gradient, ranging from 5 to 77% and were significantly negatively correlated with salinity ($P < 0.01$). Sediment organic matter was also recognized as an important factor in controlling the relative role of anammox to total N_2 production in the Yangtze estuarine and coastal zone. Overall, our data demonstrated a biogeographical distribution of anammox bacterial diversity, abundance, and activity along the estuarine salinity gradient and suggested that salinity is a major environmental control on anammox process in the estuarine and coastal ecosystems.

1. Introduction

In this century, global nitrogen (N) overload has been identified as a major environmental issue, due mainly to the widespread application of artificial N fertilizers and excessive combustion of fossil fuels [*Gruber and Galloway*, 2008; *Kim et al.*, 2014; *Hou et al.*, 2015]. Much of the anthropogenic N is delivered to the estuarine and coastal areas through river flow, groundwater discharge, and atmospheric deposition [*Jickells*, 1998; *Seitzinger*, 2008; *Diaz and Rosenberg*, 2008; *Kim et al.*, 2014], consequently exerting a serious threat to these aquatic ecosystems. Therefore, understanding of N removal processes and related microbial mechanisms is important for developing N management strategies to protect these aquatic ecosystems [*Dale et al.*, 2009; *Naeher et al.*, 2015].

Of the N removal processes, anaerobic ammonium oxidation (anammox) was recently discovered and identified as a significant pathway for reactive N removal from various natural ecosystems [*Kuypers et al.*, 2003; *Trimmer et al.*, 2005; *Wang et al.*, 2012; *Hou et al.*, 2013; *Naeher et al.*, 2015]. This N removal process, which oxidizes ammonium (NH_4^+) via reducing nitrite (NO_2^-) to form N_2 under anaerobic environments [*Mulder et al.*, 1995], is known to be mediated by chemolithoautotrophic bacteria belonging to the phylum *Planctomycetes* [*Strous et al.*, 1999; *Kartal et al.*, 2007; *Jetten et al.*, 2010]. To date, five anammox bacterial genera have been recognized, which include *Candidatus Kuenenia*, *Candidatus Brocadia*, *Candidatus Scalindua*, *Candidatus Anammoxoglobus*, and *Candidatus Jettenia* [*Strous et al.*, 1999; *Schmid et al.*, 2000; *Kartal et al.*, 2007; *Quan et al.*, 2008], and all these genera have been reported to exist in estuarine and coastal habitats [*Dale et al.*, 2009; *Fu et al.*, 2015]. Although the process of anammox is an important pathway for removing N from estuarine and coastal environments [*Dale et al.*, 2009; *Hou et al.*, 2013; *Naeher et al.*, 2015], little is known about how community dynamics and activity of anammox bacteria shift along the estuarine salinity gradient.

Salinity has been implicated as a key factor regulating anammox bacterial community composition [*Dale et al.*, 2009; *Fu et al.*, 2015] and activity [*Rich et al.*, 2008; *Koop-Jakobsen and Giblin*, 2009], as it plays an important

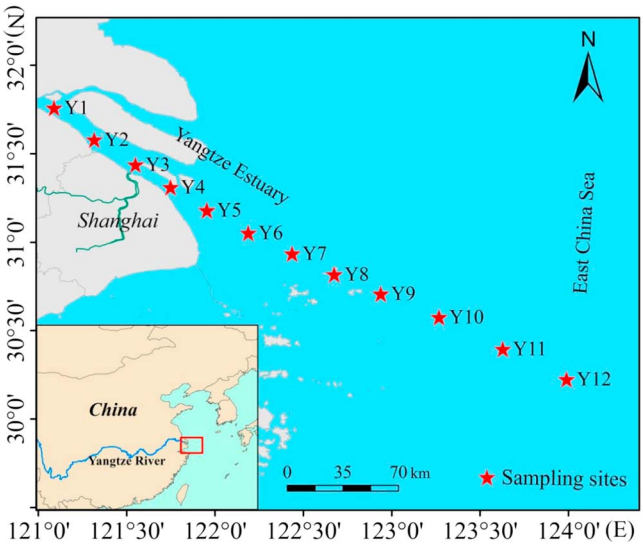

Figure 1. Study area. The figure shows the location of the Yangtze Estuary and the sampling sites during field investigations.

role in controlling the availability of N substrates in sediments [*Boynton and Kemp*, 1985; *Bernhard et al.*, 2005] and/or different anammox bacterial genera might favor different salinity niches [*Fu et al.*, 2015]. In estuarine and coastal environments, the spatially and seasonally varying mixtures of freshwater and seawater generally create a steep salinity gradient and thus presents a unique environment to refine our understanding of salinity effects on the anammox process.

In the present study, the Yangtze estuarine and coastal zone was selected as the study area. The Yangtze River plays an important role in the global biogeochemical cycles, as it is the largest river over the Euro-Asian continent, and is ranked third, fourth, and fifth in river length, sediment discharge, and freshwater discharge, respectively, around the world [*Hou et al.*, 2013; *Deng et al.*, 2015]. In recent decades, an increasing load of anthropogenic N has been discharged into the Yangtze estuarine and coastal zone due to human activities [*Chai et al.*, 2006; *Hou et al.*, 2013], consequently resulting in severe eutrophication in the estuary and adjacent coastal areas [*Chai et al.*, 2006]. Therefore, the microbe-driven N removal processes are one of the major concerns in the Yangtze estuarine and coastal ecosystems. Although the anammox importance in N removal has been recognized in recent years, few research works have investigated dynamics of anammox bacteria and their activities simultaneously along the estuarine salinity gradient. In this study, we examined the biodiversity, abundance, and distribution of anammox bacteria in the Yangtze estuarine and coastal sediments over a salinity range of 0.1–33.8 using molecular methods. Activity of anammox bacteria along the salinity gradient was also measured using sediment-slurry experiments combined with N isotope-tracing technique. Additionally, we estimated the contribution of anammox process to total N_2 fluxes and explored how it was shifted along the estuarine salinity gradient. This work may improve our understandings of the microbial N transformations in the estuarine and coastal ecosystems.

2. Materials and Methods

2.1. Field Sampling

The study sites were located in the Yangtze Estuary and adjacent coastal areas (Figure 1). In the present study, 12 sites (Y1 to Y12) were selected along the Yangtze estuarine salinity gradient, and field surveys were performed in March (dry season) and July (flood season) 2015, respectively. The water depth of the study area varied from 5 to 60 m. A marked salinity gradient (0.1–33.8) was observed along the sampling transect. Based on the salinity distribution, these sampling sites were divided into three categories: low-salinity sites (0.1–0.5, Y1 to Y4), midsalinity sites (3.9–22.3, Y5 to Y8), and high-salinity sites (27.6–33.8, Y9 to Y12). Surface sediment (0–5 cm) of each site was sampled in triplicate by subcoring a box corer (50 cm × 50 cm × 50 cm) with PVC tubes (7.2 cm diameter and 5 cm length). Near-bottom water (0.5 m above the sediment) was also collected from each site during the field surveys. Upon return to the laboratory, surface sediment of each site was immediately and completely mixed under a helium condition to form one composite sample. After that, one fraction of the sediment sample was stored at −80°C for subsequent genomic DNA extraction and molecular analysis, while the remaining sediment was preserved at 4°C for sediment physicochemical analyses and anammox rate measurements.

2.2. Determination of Environmental Parameters

Salinity of the overlying water was determined with YSI Model 30 salinity meter (YSI, Yellow Springs Instrument), which was calibrated using conductivity standards of 1 mS cm^{-1} (YSI Catalogue #3167) for freshwater, 10 mS cm^{-1} (YSI Catalogue #3168) for brackish water, and 50 mS cm^{-1} (YSI Catalogue #3169) for seawater. Grain size of the sediment was analyzed with a laser granulometer (Beckman Coulter LS13320, USA). Water content of sediment was calculated based on the weight loss of a known amount of fresh sediment, which was dried at 60°C to a constant value [*Hou et al*., 2013]. Exchangeable NH_4^+ and nitrate (plus nitrite, NO_x^-) were extracted with 2 M KCl from fresh sediments, and then spectrophotometrically determined using nutrient analyzer (SAN plus, *Skalar Analytical* B.V., Netherlands) with detection limits of 0.1 μM for NO_x^- and 0.5 μM for NH_4^+ [*Hou et al*., 2013]. Dissolved NH_4^+ and NO_x^- in the overlying water were also determined with the nutrient analyzer. Sediment sulfide concentration was analyzed by a microelectrode (Unisense H_2S-100) connected to a picoampere meter (Unisense Picometer PA2000). Fe(II) was extracted from fresh sediments with 0.5 M HCl, and then quantified by the ferrozine colorimetric method [*Roden and Lovley*, 1993]. Sedimentary organic matter (OM) was determined by $K_2Cr_2O_7$ oxidation method [*Wang et al*., 2012]. All these physicochemical characteristics were determined in triplicate in this study. Detailed information on the parameters of both sediment and overlying water samples is given in Table S1 in the supporting information.

2.3. DNA Extraction and Gene Amplification

Total genomic DNA of each sampling site was extracted from approximately 0.25 g of the homogenized sediments using Powersoil™ DNA Isolation Kits (MOBIO, USA) according to the instructions from the manufacturer. Duplicate extracts were pooled for the down-stream molecular analyses. Anammox bacterial 16S rRNA gene was amplified using a nested polymerase chain reaction (PCR) approach as previously described [*Hou et al*., 2013]. In brief, the initial PCR amplification was conducted using primers PLA46f-1390r, followed by a second amplification with Amx368f-Amx820r primer set [*Schmid et al*., 2000, 2005]. During PCR amplifications, negative controls without template DNA were always included. Appropriately sized PCR fragments were separated through electrophoresis, and then purified with Gel Advance-Gel Extraction system (Viogene, China). Subsequently, these genomic fragments were cloned with the TOPO-TA cloning kit (Invitrogen, USA), and clones were selected randomly for further sequencing analysis. More detailed information on gene amplification is shown in Table S2.

2.4. Phylogenetic Analyses

Selected clones were sequenced on an ABI Prism genetic analyzer (Applied Biosystems, Canada). The qualified nucleic acid sequences with more than 97% identities were defined as one operational taxonomic unit (OTU) by software Mothur (version 1.35.1) using the furthest neighbor method [*Schloss et al*., 2009]. The closest reference sequences were selected using the nucleotide blast program (http://blast.ncbi.nlm.nih.gov/Blast.cgi). The qualified sequences and their closest relatives were aligned using ClustalX software (version 2.1) [*Thompson et al*., 1997]. MEGA 5.03 program was then used for the construction of neighbor-joining phylogenetic tree [*Tamura et al*., 2007]. The topological confidence of the constructed tree was assessed by conducting 1000 bootstrap replicates. The unique clone sequences obtained in the present study have been deposited in GenBank, with accession numbers of KU217474–KU218396.

2.5. Quantitative PCR Assay

Real-time quantitative PCR (qPCR) was conducted in triplicate using the SYBR green method with primers AMX-808-F and AMX-1040-R [*Hamersley et al*., 2007] on an ABI 7500 Sequence Detection System (Applied Biosystems, Canada; Table S2). Plasmids carrying the anammox bacterial 16S rRNA gene were extracted from the *Escherichia coli* hosts using a Plasmid Mini Preparation Kit (Tiangen, China). Plasmid DNA concentrations were determined with a Nanodrop-2000 Spectrophotometer (Thermo, USA). Standard curve was then constructed using gradient dilutions of plasmids containing anammox bacterial 16S rRNA gene with known copy numbers. Melting curve analysis, as well as gel electrophoresis, was performed to confirm the qPCR amplifying specificity, and thus to lower the possibility of over-estimation. In addition, negative controls were included in all amplification reactions. Based on the above constructed standard curve, anammox bacterial 16S rRNA gene abundance was quantified, and then converted into copies per gram of dry sediment, assuming that the extraction efficiency of DNA was 100%.

Table 1. Diversity Characteristics of Anammox Bacterial 16S rRNA Gene Clone Libraries

Seasons	Sites	No. of Clones	OTUs[a]	Chao1[b]	Shannon-Wiener[c]	1/Simpson[d]	Coverage (%)[e]
July	Y1	54	11	11.3	1.98	5.7	97.1
	Y2	58	23	24.3	2.91	18.4	94.8
	Y3	55	18	19.8	2.65	14.9	91.1
	Y4	59	19	19.7	2.71	15.1	96.6
	Y5	60	14	14.1	2.06	4.8	99.1
	Y6	58	11	11.0	1.52	2.6	100.0
	Y7	60	17	17.0	2.68	15.7	100.0
	Y8	59	18	18.2	2.73	16.5	99.1
	Y9	60	13	13.2	2.25	8.4	98.5
	Y10	56	15	15.0	2.53	12.9	100.0
	Y11	62	12	12.0	2.08	6.2	100.0
	Y12	57	17	19.1	2.44	9.7	89.0
March	Y1	51	12	12.0	1.84	3.7	100.0
	Y2	51	20	22.6	2.78	18.5	88.5
	Y3	57	15	15.1	2.12	4.9	99.3
	Y4	58	21	22.7	2.80	16.4	92.6
	Y5	53	11	12.0	1.93	5.1	91.7
	Y6	50	4	4.0	0.94	2.1	100.0
	Y7	53	8	8.0	1.79	5.3	100.0
	Y8	52	12	12.1	1.94	4.9	98.8
	Y9	51	13	14.2	1.89	4.3	91.5
	Y10	54	15	15.4	2.35	9.1	97.6
	Y11	54	15	15.0	2.39	8.7	100.0
	Y12	55	16	16.4	2.37	7.7	97.4

[a]OTUs are defined at 3% nucleotide acid divergence.
[b]Nonparametric statistical predictions of total richness of OTUs based on distribution of singletons and doubletons.
[c]Shannon diversity index. A higher number represents more diversity.
[d]Reciprocal of Simpson's diversity index. A higher number represents more diversity.
[e]Percentage of coverage: percentage of observed number of OTUs divided by Chao1 estimate.

2.6. Measurement of Nitrogen Transformation Rates

Potential rates of anammox and denitrification were measured using sediment-slurry experiments in combination with N isotope-tracing technique, as previously described [*Risgaard-Petersen et al*., 2004; *Engström et al*., 2005]. In brief, sediment slurries were prepared with helium-purged site water and fresh sediments at a volume ratio of 5:1 (water/sediment) and then transferred into 12 mL helium-flushed Exetainer vials (Labco, High Wycombe, Buckinghamshire, UK). The slurries were subsequently preincubated at in situ temperature for over 24 h to consume the ambient NO_x^- and O_2. These vials were separated into three groups after preincubation, which were spiked with helium-purged stock solutions of (1) $^{15}NH_4^+$ (^{15}N at 99.6%), (2) $^{15}NH_4^+ + {}^{14}NO_3^-$, and (3) $^{15}NO_3^-$ (^{15}N at 99%), respectively. The resulting final concentrations of ^{15}N were approximately 100 μM in each vial. The incubation was inhibited by injecting 300 μL of 50% $ZnCl_2$ solution after 8 h [*Hou et al*., 2013]. The concentrations of $^{29}N_2$ and $^{30}N_2$ produced during incubation were determined using membrane inlet mass spectrometry [*An and Gardner*, 2002; *Yin et al*., 2014]. Potential rates of both anammox and denitrification were quantified with the methods described in *Thamdrup and Dalsgaard* [2002] and *Trimmer et al*. [2003] and expressed on a dry sediment weight basis.

2.7. Statistical Analysis

The biodiversity indices (Shannon-Wiener and Simpson) and species richness Chao1 estimator were calculated for the clone libraries with Mothur program (version 1.35.1) [*Schloss et al*., 2009]. Clone library coverage was estimated by the percentage of the observed OTU number divided by Chao1 estimator [*Mohamed et al*., 2010]. Correlations between anammox bacterial community structure and environmental variables were examined with the canonical correspondence analysis (CCA) using Canoco 4.5 software [*ter Braak and šmilauer*, 2002]. Community classifications were conducted with the principal coordinates analysis (PCoA) using Qiime 1.9.0 [*Caporaso et al*., 2010]. The distance between clone libraries was calculated by UniFrac test, and the *P* value was corrected by multiple comparisons using the Bonferroni correction (*P* value was multiplied by the number of pairwise comparisons performed) [*Lozupone et al*., 2011]. Pearson and partial

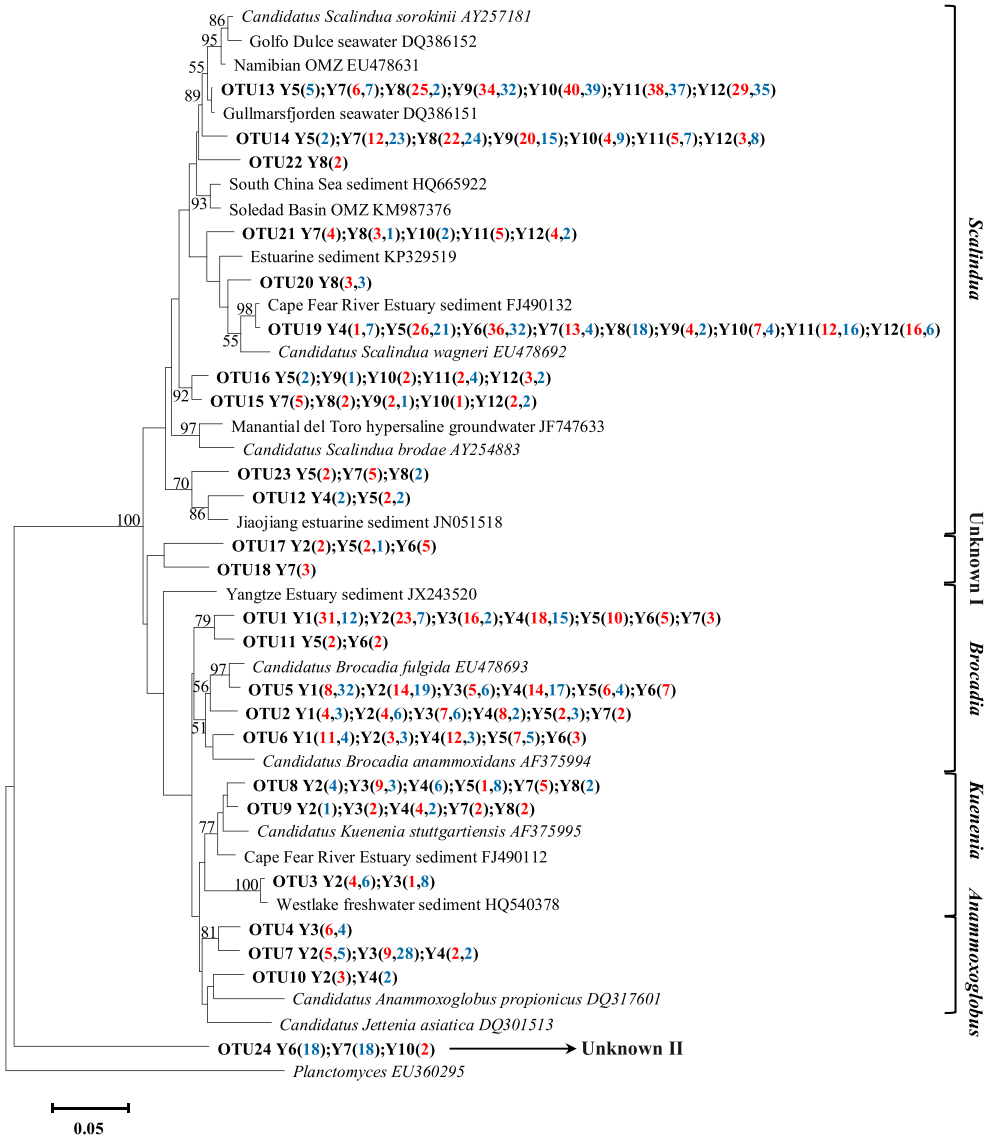

Figure 2. Neighbor-joining phylogenetic tree of anammox bacterial 16S rRNA gene sequences. Bootstrap values greater than 50% of 1000 resamplings are shown near nodes. The scale indicates the number of nucleotide substitutions per site. GenBank accession numbers are shown for sequences from other studies. Numbers in parentheses followed each OTU indicate the number of sequences recovered from each sampling sites. OTUs are defined at 6% nucleotide acid divergence. The July samples are in *red front*, while the March samples are in *blue*.

correlation analyses were conducted using SPSS (version 16.0) to examine the correlations among environmental factors, anammox bacterial activity and abundance. In addition, a one-way analysis of variance (ANOVA) was performed to compare spatial and seasonal variations in anammox dynamics.

3. Results

3.1. Occurrence and Diversity of Anammox Bacteria

Anammox bacterial communities in the sediments along the salinity gradient of the Yangtze estuarine and coastal zone were successfully detected with the nested PCR method. The retrieved sequences of anammox bacterial 16S rRNA gene were analyzed by Blast search, confirming that all of the qualified clones represented anammox-like sequences. In this study, 1337 sequences were obtained from the 24 constructed clone libraries along the salinity gradient, which represented 923 unique sequences and 110 OTUs at a 3%

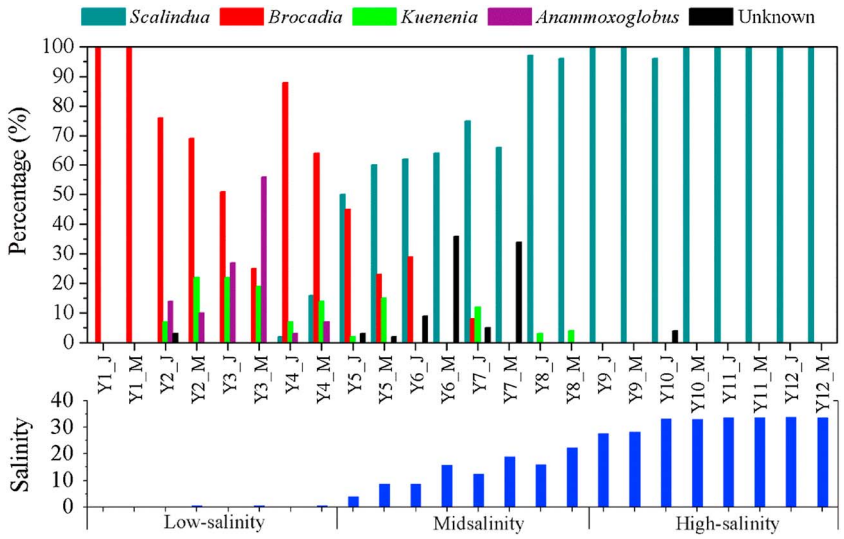

Figure 3. The community compositions and distributions of anammox bacteria in the surface sediments of the Yangtze estuary and coastal zone along the salinity gradient. J denotes July; M denotes March. The salinity ranges for low-salinity, midsalinity and high-salinity sites are 0.1–0.5, 3.9–22.3, and 27.6–33.8, respectively.

nucleotide acid divergence (Table 1). Rarefaction analysis indicated that most of the observed anammox bacterial sequences were represented in the constructed clone libraries (Figure S1 in the supporting information), which was in consistence with the estimated coverage values (89–100%; Table 1). On the basis of Shannon-Wiener and Chao1 diversity indices at a 3% distance level, low-salinity sites Y2 and Y4 showed the maximal OTU diversity, while the minimal OTU diversity appeared at the midsalinity site Y6. However, at 6% distance level (genus level, the five known anammox genera were separated at this level), midsalinity sites Y5 and Y7 exhibited the highest diversity and the high-salinity sites Y9 and Y10 showed the lowest diversity (Table S3). In addition, anammox bacteria exhibited relatively higher diversity from sites Y2 to Y7 (except for site Y6), with salinity ranging from 0.1 to 18.9, compared with the other sampling sites at 6% nucleotide acid divergence (Table S3).

3.2. Microbial Community and Spatial Distribution of Anammox Bacteria

Phylogenetic analysis indicated four known genera of anammox bacteria, including *Candidatus Scalindua*, *Kuenenia*, *Brocadia*, and *Anammoxoglobus*, and two unknown anammox-like groups were observed in the Yangtze estuarine and coastal sediments (Figure 2). *Brocadia*, *Anammoxoglobus*, and *Kuenenia* were observed to coexist at the low-salinity sites (Y1–Y4), occupying 71%, 15%, and 11% of the total low-salinity site clones, respectively. The remaining 3% of the sequences acquired from the low-salinity sites (only observed at Y4) were affiliated with *Scalindua* (Figures 2 and 3). Most of the low-salinity sites were dominated by *Brocadia* genus (*Brocadia fulgida* and *Brocadia anammoxidans*, with 94–98% sequence identity), which accounted for 51–100% of the obtained sequences in each clone library. The only exception was observed at site Y3 during the March investigation, which was dominated by *Anammoxoglobus* genus (occupying 56% of the clone sequences), with 92–93% sequence similarity. At the midsalinity sites (Y5–Y8), *Scalindua*, *Brocadia*, and *Kuenenia* were detected to coexist, which accounted for 71%, 14%, and 4% of the total midsalinity sites clones, respectively. The remaining 11% of the sequences obtained from the midsalinity sites were affiliated with the unknown anammox-like group (sequence similarity $<$92% compared with the known anammox genera). In contrast to the low-salinity sites, all the midsalinity sites were dominated by genus *Scalindua* (with 94–99% sequence identity), which occupied 50–97% of the sequences in each clone libraries. At the high-salinity sites (Y9–Y12), however, the observed sequences were solely (100%) grouped into *Scalindua* genus (95–99% sequence identity), with only two sequences (obtained from site Y10 during the July sampling and accounting for only 0.4% of the total high-salinity site clones) belonging to the unknown anammox-like assemblage. The retrieved anammox bacterial 16S rRNA gene clones in the Yangtze estuarine and adjacent coastal zone were affiliated closely with sequences obtained from other estuarine and marine environments including the Cape Fear River estuarine sediment [*Dale et al.*, 2009], Jiaojiang estuarine sediment [*Hu et al.*, 2012], Gullmarsfjorden seawater [*Schmid et al.*, 2007], and

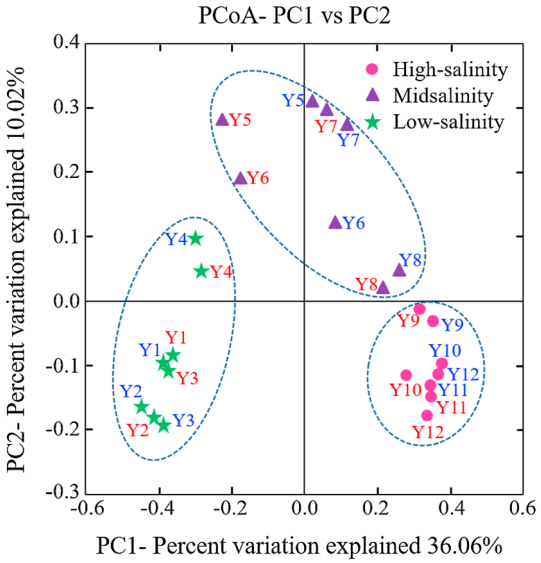

Figure 4. The UniFrac unweighted PCoA analysis of the anammox bacterial assemblages as revealed by the 16S rRNA gene sequences. The first two principal coordinate axes (PC1 and PC2) are shown. The July samples are in *red front*, while the March samples are in *blue*.

South China Sea sediment [*Li et al.*, 2013], and with sequences from hypersaline groundwater ecosystems and lacustrine sediments [*Shen et al.*, 2011], with 95–100% sequence identity (Figure 2).

Along the salinity gradient of the Yangtze estuarine and coastal zone, obvious geographical specific distributions of anammox bacterial communities were revealed by the UniFrac PCoA analysis (Figure 4). Approximately 46.08% of the anammox bacterial community variabilities were explained by the first two principal coordinate axes (PC1 and PC2). The plot of the first two axes showed that anammox bacterial assemblages along the salinity gradient fell into three groups. Anammox communities at sites Y1 to Y4 were grouped together and fell into the low-salinity group, which shared the freshwater anammox bacterial characteristics. Anammox communities at sites Y9 to Y12 possessed obvious marine features and belonged to the high-salinity group. The remaining anammox bacterial communities at sites Y5 to Y8, where freshwater and seawater mixed, fell into the midsalinity group. The observed high spatial heterogeneity in the anammox bacterial community compositions was further confirmed by the UniFrac distance matrix. The anammox communities acquired from the low-salinity sites (Y1–Y3) were observed to be significantly different from those retrieved from relatively higher-salinity sites (Y6–Y12) ($P < 0.01$; Table S4). CCA analysis was also conducted to reveal the potential relationships of anammox bacterial

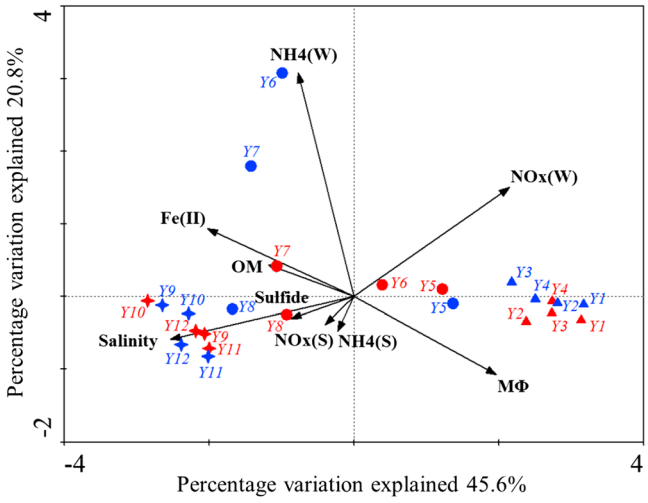

Figure 5. CCA ordination plots for the first two principal dimensions showing the relationship between environmental factors and the anammox bacterial communities. Correlations between environmental variables and CCA axes are represented by the length and angle of arrows. MΦ, NO_x(W), NO_x(S), NH_4(W), NH_4(S), and OM represent sediment mean size, NO_x^- (nitrite plus nitrate) in overlying water, NO_x^- in the sediment, NH_4^+ in overlying water, NH_4^+ in the sediment, and organic matter, respectively. The *red* and *blue* symbols represent July and March samples, respectively. Samples obtained from low-salinity, midsalinity, and high-salinity sites are shown as up-triangle, circle, and star, respectively.

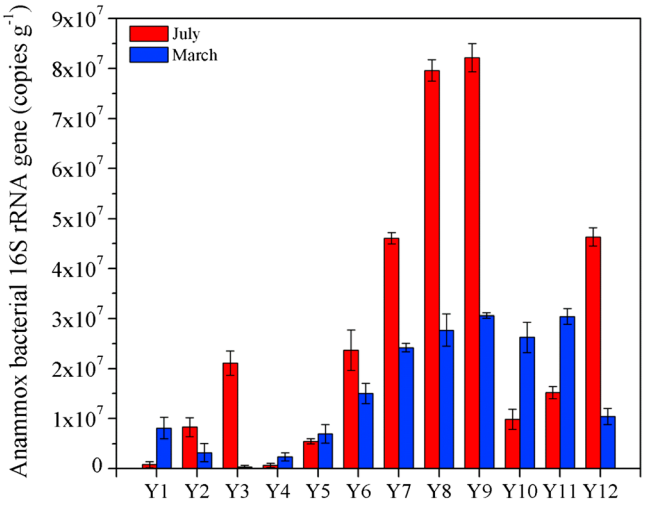

Figure 6. The spatiotemporal variations of anammox bacterial abundance targeting on 16S rRNA gene at each site. The vertical bars indicate standard error ($n = 3$).

communities with environmental factors (Figure 5). The first two CCA axes explained 66.4% of the cumulative variation of the anammox community-environment relationship. These results confirmed that salinity did have a significant relationship with the distribution and composition of the anammox communities ($P = 0.002$, 499 Monte Carlo permutations) and solely provided 42.5% of the total CCA explanatory power. Additionally, the structure and distribution of anammox bacterial communities were also correlated with overlying water NO_x^- and NH_4^+, sediment particle size, and Fe(II) content ($P < 0.05$, 499 Monte Carlo permutations).

3.3. Abundance of Anammox Bacteria

In this study, the melting-curve analyses confirmed that the fluorescent signals were derived from the specific PCR products in the process of qPCR quantifications. A significant linear relationship ($R^2 = 0.9991$), with 99% amplification efficiency, was obtained between the $\log_{10}$ values of the standard plasmid DNA concentration (1.72×10^2 to 1.72×10^9 copies μL^{-1}) and the associated threshold cycles (Ct). The qPCR results showed that the abundance of anammox bacteria exhibited a geographically heterogeneous distribution pattern along the salinity gradient of the Yangtze estuarine and coastal zone (Figure 6). The abundance of anammox bacterial 16S rRNA genes varied between 3.67×10^5 and 8.22×10^7 copies g^{-1}, and the highest number of copies was recorded at site Y9 in July, while the lowest gene copy number was detected at site Y3 in March. In general, the anammox bacteria were more abundant at the midsalinity and high-salinity sites (5.46×10^6–8.22×10^7 copies g^{-1}) than at the low-salinity sites (3.67×10^5–2.11×10^7 copies g^{-1}) (one-way ANOVA, $P < 0.01$). Anammox bacterial abundance was positively correlated to the change in salinity ($P < 0.05$; Table S5), as revealed by the Pearson correlation analyses. In addition, the spatial variation of anammox bacterial abundance was also

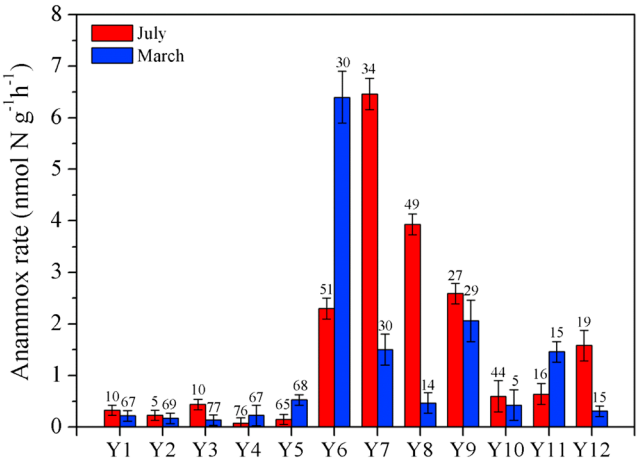

Figure 7. The spatiotemporal variations of anammox activities and the contribution of anammox to total N_2 production at each site. The vertical bars indicate standard error ($n = 3$). The numbers on the top of each column represent the contributions of anammox to total N_2 production (%) at each sampling site.

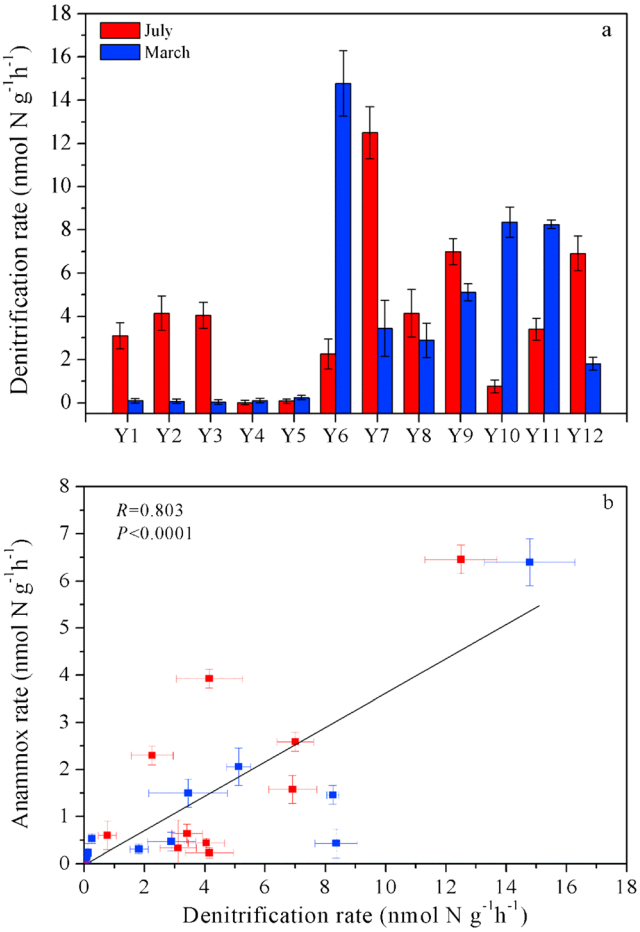

Figure 8. (a) The spatiotemporal variations of denitrification rates at each site and (b) their correlation with anammox rates. *Red*: July; *blue*: March. The error bars indicate SD ($n = 3$).

related significantly to the sediment grain size, overlying water NO_x^- concentrations, and sediment NH_4^+, sulfide, Fe(II), and OM contents ($P < 0.05$). The average abundance of anammox bacteria was slightly higher in July (2.83×10^7 copies g^{-1}) than in March (1.55×10^7 copies g^{-1}), but no significant seasonal variation was found in the study area (one-way ANOVA, $P > 0.05$).

3.4. Anammox Rate and Contribution to N_2 Production

Anammox potential activity and its contribution to total N_2 production were estimated by sediment-slurry incubations in combination with ^{15}N tracing technique. In the present study, no significant accumulation of ^{15}N-labeled gases ($^{29}N_2$ and/or $^{30}N_2$) was measured (one-way ANOVA, $P > 0.05$) during incubations spiked with only $^{15}NH_4^+$, indicating that ambient NO_x^- were consumed within the preincubation. Significant production of $^{29}N_2$ was detected when both $^{15}NH_4^+$ and $^{14}NO_3^-$ were added (one-way ANOVA, $P < 0.05$), but no significant production of $^{30}N_2$ was detected (one-way ANOVA, $P > 0.05$). This result implied that anammox activity occurred at all the sampling sites. Significant production of both $^{29}N_2$ and $^{30}N_2$ was detected in incubation vessels spiked with only $^{15}NO_3^-$ (one-way ANOVA, $P < 0.05$). Thereby, the potential activities of both anammox bacteria and denitrifiers could thereby be quantified, on the basis of the $^{15}NO_3^-$ incubations.

In this study, the estimated activity of anammox bacteria in the sediments ranged from 0.08 to 6.46 nmol N g^{-1} h^{-1} along the salinity gradient (Figure 7), with a distinct spatial heterogeneity (one-way ANOVA, $P < 0.05$). The highest rate of anammox was observed at the midsalinity site Y7 during the July sampling, whereas the lowest anammox activity occurred at the low-salinity site Y4 in July. In general, higher activities of anammox bacteria were recorded at the midsalinity and high-salinity sites than at the low-salinity sites (one-way ANOVA, $P < 0.05$), with mean values of 1.96 and 0.23 nmol N g^{-1} h^{-1}, respectively. However, the rates of anammox were not significantly related to salinity, but to the sediment grain size, overlying water NH_4^+, and sediment Fe(II), sulfide, and OM ($P < 0.05$). In addition, a significant linear relationship was found between the anammox activity and associated bacterial abundance ($R = 0.553$, $P = 0.005$; Figure S2). Although no significant seasonal variations in anammox activities were observed (one-way ANOVA, $P > 0.05$), anammox bacteria tended to be more active in July than in March (except for sites Y4, Y5, Y6, and Y11), with respective average rates of 1.61 and 1.16 nmol N g^{-1} h^{-1}. Additionally, the cell-specific anammox rates were estimated between 0.4 and 10.2 fmol N $cell^{-1}$ d^{-1}, assuming that each anammox bacterium only contained one targeted gene copy and had equal activity. The observed cell-specific anammox activity was significantly associated with overlying water NH_4^+ and NO_3^- ($P < 0.05$). However, it was negatively, although insignificantly, correlated with salinity ($R = -0.323$, $P = 0.124$).

Denitrification rates were also determined in the sediments along the Yangtze estuarine salinity gradient. The measured denitrification activities varied from 0.02 to 14.78 nmol N g^{-1} h^{-1}, which were strongly correlated with anammox rates ($R = 0.803$, $P < 0.0001$; Figure 8). Meanwhile, compared with denitrification, the anammox process was estimated to contribute 5–77% to the total N loss along the salinity gradient (Figure 7). The relative importance of anammox was also observed to significantly and negatively correlate with salinity and sediment OM content ($P < 0.01$).

4. Discussion

Geographical distributions and seasonal variations of the anammox bacterial communities, abundance, and activities were examined along the salinity gradient of the Yangtze estuarine and coastal zone. High anammox bacterial biodiversity (*Scalindua*, *Brocadia*, *Anammoxoglobus*, *Kuenenia*, and two unknown anammox-like groups) was evidenced by 16S rRNA gene phylogenetic analyses along the estuarine salinity gradient (Figure 2). In contrast, relatively lower diversity of anammox bacteria was reported in lacustrine, riverine, and marine environments, which is mainly restricted to *Brocadia* or *Scalindua* genus [*Zhang et al*., 2007; *Yoshinaga et al*., 2011; *Hu et al*., 2012; *Hou et al*., 2013]. The higher anammox bacterial diversity in the estuarine ecosystem was likely attributed to the land-sea interaction, which is in agreement with the previous studies [*Dale et al*., 2009; *Hou et al*., 2013; *Fu et al*., 2015]. The Yangtze River possesses the largest discharge rate in China, with an average runoff of approximately 29,000 m^3 s^{-1} [*Beardsley et al*., 1985; *Yang et al*., 2015; *Yuan et al*., 2016], which transports huge amount of freshwater into the adjacent sea. Therefore, a great deal of terrestrial materials have also been brought into the estuarine and coastal regions. Meanwhile, tidal dynamics can give rise to rhythmic material exchanges between the estuary and sea [*Zheng et al*., 2016]. During these interactions, anammox species originated from both marine and terrestrial environments may be blended by tidal current and river runoff in the estuarine ecosystem, thus enhancing its anammox bacterial biodiversity [*Hou et al*., 2013].

Distinctive shift in anammox bacterial communities was detected along the salinity gradient (Figures 3 and 4 and Table S4), which might be due to different salinity tolerance of diverse anammox genera [*Fu et al*., 2015]. In the present study, *Brocadia* genus dominated the anammox assemblages at the head of the Yangtze Estuary, where salinity was relatively low, which averagely occupied 71% of observed sequences in each clone library. With the increasing salinity, the proportion of *Brocadia* in anammox assemblages decreased, and it disappeared when salinity was higher than 12.5. These results provided additional evidence for the previous statement that *Brocadia* is favored to grow in freshwater or/and brackish environments [*Hu et al*., 2012; *Hou et al*., 2013]. In contrast, *Scalindua* genus, which is reported to have a high tolerance to salinity [*Schmid et al*., 2007], was not detected at the low-salinity sites Y1–Y3 (salinity: 0.1–0.5), and its proportion increased from less than 15% at site Y4 to approximately 100% at sites where salinity was higher than 22.3. These results suggested that *Scalindua* was not only "highly tolerant to salinity" [*Fu et al*., 2015], but also, it was halophilic and might adapt better in higher salinity environments. *Kuenenia* was observed to occur at the low-salinity and midsalinity sites where salinity ranged from 0.1 to 22.3. *Anammoxoglobus*, however, was only observed at the low-salinity sites Y2–Y4 (salinity: 0.1–0.5). Therefore, salinity might be a key environmental variable in controlling the biogeographical distribution of anammox bacteria [*Hou et al*., 2013]. This statement was further supported by the CCA analysis (Figure 5), confirming that salinity did significantly correlate with the distribution and composition of the anammox communities.

Two unknown anammox-like groups were obtained in the present study (Figure 2). Approximately 93% of the unknown potential anammox clones were retrieved from the midsalinity sites (Y5–Y7) where freshwater mixed with seawater. These sites were also located in the turbidity maximum zone of the Yangtze Estuary, and thus, the anammox community might be more complex to adapt to this comprehensive hydrological and biogeochemistry conditions [*Yang et al*., 2014]. These unknown anammox-like groups observed at the midsalinity sites were outside the "anammox bacterial cluster" with <92% sequence similarities and had no close representatives among cultivated organisms; thus, the possibility that they represent yet-uncultivated anammox microbe cannot be excluded.

Anammox bacterial 16S rRNA gene abundance in the sediments was observed between 3.67×10^5 and 8.22×10^7 copies g^{-1} along the estuarine salinity gradient (Figure 6), which is relatively higher than that observed in the Cape Fear River Estuary (1.3×10^5–8.4×10^6 copies 16S rRNA gene g^{-1}) [*Dale et al*., 2009],

Jiaozhou Bay (3.5×10^5–5.9×10^6 copies *hzo* gene g^{-1}) [*Dang et al.*, 2010], and Pearl Estuary (4.22×10^5–2.55×10^6 copies 16S rRNA gene g^{-1}) [*Fu et al.*, 2015]. However, an even higher anammox bacterial abundance, ranging from 1.3×10^6 to 2.0×10^9 copies *hzsB* gene g^{-1}, was reported in the riparian sediments of the Pearl Estuary [*Wang et al.*, 2012]. In the present study, significantly low anammox bacterial abundance was detected at the upstream of the estuary (sites Y1–Y5, 3.67×10^5–2.11×10^7 copies g^{-1}), where salinity was low (0.1–8.6), compared with the higher salinity sites (Y6–Y12, 9.81×10^6–8.22×10^7 copies g^{-1}) (one-way ANOVA, $P < 0.05$). In our investigation, the significant increase in the anammox bacterial abundance with salinity ($R = 0.452$, $P = 0.027$) might be attributed to the fact that more cations and anions contained in seawater could exchange NH_4^+ and NO_2^- from sediments [*Boatman and Murray*, 1982; *Boynton and Kemp*, 1985; *Rysgaard et al.*, 1999; *Bernhard et al.*, 2005; *Wang and Gu*, 2014]. As NH_4^+ and NO_2^- are the substrates for anammox bacteria, the release of NH_4^+ and NO_2^- might favor anammox bacteria and thus lead to the higher anammox bacterial abundance [*Wang and Gu*, 2014]. Significant correlation was also detected between anammox bacterial numbers and salinity in the Cape Fear River Estuary where salinity ranged between 0 and 9.9 [*Dale et al.*, 2009]. In this study, however, the highest abundance of anammox bacteria (8.22×10^7 copies g^{-1}) occurred at site Y9, where salinity was 27.6–28.3, after which the abundance decreased with increasing salinity (33.1–33.8). This distribution pattern implicated that salinity at a certain level (>29 in this study) may cause a physiological stress on the metabolism of anammox cell. Additionally, significant linear correlations between the anammox bacterial abundance and denitrification rates were observed ($P < 0.05$), implying that denitrifiers might provide anammox bacteria with NO_2^- substrate and thus stimulate their proliferation [*Thamdrup and Dalsgaard*, 2002; *Trimmer et al.*, 2005; *Hou et al.*, 2013].

The detected rates of anammox in this study (0.08–6.46 nmol N g^{-1} h^{-1}) are relatively higher than those reported in other estuarine sediments, including the Pearl Estuary (0.04–1.4 nmol N g^{-1} h^{-1}) [*Wang et al.*, 2012], Seine Estuary (0.6–1.3 nmol N g^{-1} h^{-1}) [*Naeher et al.*, 2015] and Cape Fear River Estuary (0.13–1.32 nmol N g^{-1} h^{-1}) [*Dale et al.*, 2009], which are in agreement with the relatively higher anammox bacterial abundance in our investigation (Figures 6 and 7). Specific cellular anammox activities were calculated between 0.4 and 10.2 fmol N $cell^{-1}$ d^{-1}, which are comparable to the previous reported values (0.26–20 fmol N $cell^{-1}$ d^{-1}) [*Strous et al.*, 1999; *Kuypers et al.*, 2003; *Wang et al.*, 2012; *Hou et al.*, 2013]. Although salinity shift had significant influences on the community structure and abundance of anammox bacteria, no significant linear correlation was detected between salinity and anammox rates in the present study. The highest rate of anammox occurred at the midsalinity sites, rather than at the high-salinity sites. This result further implied that salinity at high levels might cause physiological stresses on anammox activity, which was further supported by the negative correlation between the specific cellular anammox activity and salinity. Although the presence of anammox bacteria does not indicate that they are active in situ, functional bacterial abundances often reflect recent process activities [*Petersen et al.*, 2012; *Papaspyrou et al.*, 2014]. This statement was supported by the significant linear relationships between abundance and activities of anammox bacteria in the present study. Additionally, significant linear relationship was also observed between anammox and denitrification activities (Figure 8), further supporting the hypothesis that anammox and denitrification may be coupled [*Hou et al.*, 2013; *Brin et al.*, 2014].

In the present study, Fe(II) was observed to significantly and positively correlate with both anammox bacterial abundance and activity ($P < 0.05$). We postulated that this pattern might be attributed to the process of anaerobic ammonium oxidation coupled with Fe(III) reduction, which continuously generates Fe(II) and contributes to N removal [*Li et al.*, 2015]. At the same time, NO_2^- and NO_3^- can also be generated during this process, and thus might benefit anammox bacteria and lead to higher anammox bacterial abundance and activity [*Li et al.*, 2015]. A negative correlation between sulfide and anammox bacterial abundance and activity was expected, because sulfide might be an inhibitor for anammox process [*Jensen et al.*, 2008]. In contrast, Pearson correlation analysis showed significant positive relationship between them ($P < 0.05$). However, when we used partial correlation analysis to control for Fe(II), which was significantly and positively linked with sulfide, the correlations of sulfide with anammox bacterial abundance and activity were insignificant ($P > 0.05$). We postulated that the non-negative correlations between them were likely due to the binding of sulfide with Fe(II), because the production of iron sulfide (FeS) might decrease the bioavailability of free sulfide [*Deng et al.*, 2015].

Compared to denitrification, the process of anammox was estimated to contribute 5–77% to the total N_2 production (Figure 7), indicating that this microbial process played a significant role in reactive N removal from

the Yangtze estuarine and coastal zone. In this study, the estimated contributions of anammox process to total N_2 production are higher than those reported in other studies (0.5–33%) [*Trimmer et al*., 2003; *Dale et al*., 2009; *Wang et al*., 2012; *Teixeira et al*., 2014; *Naeher et al*., 2015; *Plummer et al*., 2015], which might be attributed to the lower concentrations of OM at the sampling sites (0.02–0.59%) compared with other studies (0.4–11.8%) [*Wang et al*., 2012; *Teixeira et al*., 2014; *Brin et al*., 2014]. Anammox, as an autotrophic process, does not directly need organic carbon source of electrons, whereas denitrification is a heterotrophic process in which organic carbon is required. Thus, organic matter might be an important factor in controlling the relative contributions of anammox and denitrification processes to the total N_2 production [*Gameron and Schipper*, 2010; *Deng et al*., 2015; *Plummer et al*., 2015]. In fact, this hypothesis was supported in the present study by the results that the relative contribution of anammox to total N_2 fluxes was significantly and negatively correlated with OM (R = -0.739, $P < 0.0001$). Higher contributions of anammox to total N_2 production (65–77%) were observed at sites Y1–Y5 (except for the July samples at Y1–Y3), where sediments were characterized by relatively greater sediment grain size (92–202 μm) and lower OM contents (0.02–0.19%). Significant relationship between sediment mean grain size and OM was indeed detected in the present study ($R = -0.678$, $P < 0.0001$). Thus, we further applied partial correlation analysis in which the influence from sediment mean size was controlled to investigate the effect of OM on the relative importance of anammox. This analysis showed that the correlation between the anammox contributions and OM was still significant ($P < 0.05$), confirming that OM was an important factor in controlling the relative importance of anammox process.

Despite the higher contributions to total N removal at sites Y1–Y5 (except for the July samples at Y1–Y3), the anammox activities (0.08–0.53 nmol N g^{-1} h^{-1}) at these sites were significantly lower compared with the other sampling sites (one-way ANOVA, $P < 0.05$). Thus, the observed enhancement of anammox contribution might be attributed to the inhibited denitrification rates (only 0.02–0.25 nmol N g^{-1} h^{-1}) by the shortage of OM in these sandy sediments ($R = 0.637$, $P = 0.001$). In addition, significant negative correlation between the relative importance of anammox activity and salinity was also observed ($R = -0.537$, $P = 0.007$). Further exploration of the data, using partial correlation to control for sediment mean size, Fe(II), and overlying water NO_3^- concentration, which were correlated with salinity ($P < 0.05$), in turn suggested that the relationship between the anammox contributions and salinity was significant ($P < 0.05$). Thus, we proposed that salinity might be another important factor shaping the relative contributions of both anammox and denitrification to the total N_2 production. However, more work is still required to reveal the underlying mechanism.

5. Conclusions

In the present study, diversity, abundance, and activity of anammox bacteria, and their potential contributions to total N_2 production along the salinity gradient (0.1–33.8) of the Yangtze estuarine and coastal zone, were investigated. Significant shifts in anammox bacterial community structure were detected along the estuarine salinity gradient ($P < 0.01$). Generally, a significant positive correlation was detected between salinity and the anammox bacterial abundance ($P < 0.05$). Anammox rate was significantly correlated with anammox bacterial abundance ($P < 0.01$), with the highest activity occurring at the midsalinity sites. Contributions of anammox activity to total N loss were highly variable along the salinity gradient and were significantly and negatively correlated with salinity ($P < 0.01$). These findings highlight the role of salinity as a prime environmental control on the community composition, abundance, and activity of anammox bacteria and also reinforce the importance of anammox in the removal of fixed N from estuarine and coastal ecosystems.

Acknowledgments

This study was funded by the National Natural Science Foundation of China (41322002, 41130525, 41271114, 41071135, and 41501524), the Program for New Century Excellent Talents in University, China Postdoctoral Science Foundation (2015 M581567), and the State Key Laboratory of Estuarine and Coastal Research. Thanks are given to Wayne Gardner and anonymous reviewers for their constructive suggestions on this manuscript. Data presented here can be obtained by sending a request to the corresponding authors.

References

An, S., and W. S. Gardner (2002), Dissimilatory nitrate reduction to ammonium (DNRA) as a nitrogen link, versus denitrification as a sink in a shallow estuary (Laguna Madre/Baffin Bay, Texas), *Mar. Ecol. Prog. Ser.*, *237*, 41–50.

Beardsley, R. C., R. Limburner, H. Yu, and G. A. Cannon (1985), Discharge of the Changjiang (Yangtze River) into the East China Sea, *Cont. Shelf Res.*, *4*, 57–76.

Bernhard, A. E., T. Donn, A. E. Giblin, and D. A. Stahl (2005), Loss of diversity of ammonia-oxidizing bacteria correlates with increasing salinity in an estuary system, *Environ. Microbiol.*, *7*, 1289–1297.

Boatman, C. D., and J. W. Murray (1982), Modeling exchangeable NH_4^+ adsorption in marine-sediments: Process and controls of adsorption, *Limnol. Oceanogr.*, *27*, 99–110.

Boynton, W. R., and W. M. Kemp (1985), Nutrient regeneration and oxygen-consumption by sediments along an estuarine salinity gradient, *Mar. Ecol. Prog. Ser.*, *23*, 45–55.

Brin, L. D., A. E. Giblin, and J. J. Rich (2014), Environmental controls of anammox and denitrification in southern New England estuarine and shelf sediments, *Limnol. Oceanogr.*, *59*, 851–860.
Caporaso, J. G., et al. (2010), Qiime allows analysis of high-throughput community sequencing data, *Nat. Methods*, *7*, 335–336.
Chai, C., Z. M. Yu, X. X. Song, and X. H. Cao (2006), The status and characteristics of eutrophication in the Yangtze River (Changjiang) Estuary and the adjacent East China Sea, China, *Hydrobiologia*, *563*, 313−328.
Dale, O. R., C. R. Tobias, and B. Song (2009), Biogeographical distribution of diverse anaerobic ammonium oxidizing (anammox) bacteria in Cape Fear River Estuary, *Environ. Microbiol.*, *11*, 1194–1207.
Dang, H. Y., R. P. Chen, L. Wang, L. Z. Guo, P. P. Chen, and Z. W. Tang (2010), Environmental factors shape sediment anammox bacterial communities in hyper nitrified Jiaozhou Bay, China, *Appl. Environ. Microbiol.*, *76*, 7036–7047.
Deng, F., L. Hou, M. Liu, Y. Zheng, G. Yin, X. Li, X. Lin, F. Chen, J. Gao, and X. Jiang (2015), Dissimilatory nitrate reduction processes and associated contribution to nitrogen removal in sediments of the Yangtze Estuary, *J. Geophys. Res. Biogeosci.*, *120*, 1521–1531, doi:10.1002/2015JG003007.
Diaz, R. J., and R. Rosenberg (2008), Spreading dead zones and consequences for marine ecosystem, *Science*, *321*, 926–929.
Engström, P., T. Dalsgaard, S. Hulth, and R. C. Aller (2005), Anaerobic ammonium oxidation by nitrite (anammox): Implications for N_2 production in coastal marine sediments, *Geochim. Cosmochim. Acta*, *69*, 2057–2065.
Fu, B., J. Liu, H. Yang, T. C. Hsu, B. He, M. Dai, S. J. Kao, M. Zhao, and X. H. Zhang (2015), Shift of anammox bacterial community structure along the Pearl Estuary and the impact of environmental factors, *J. Geophys. Res. Oceans*, *120*, 2869–2883, doi:10.1002/2014JC010554.
Gameron, S. G., and L. A. Schipper (2010), Nitrate removal and hydraulic performance of organic carbon for use in denitrification beds, *Ecol. Eng.*, *36*, 1588–1595.
Gruber, N., and J. N. Galloway (2008), An Earth-system perspective of the global nitrogen cycle, *Nature*, *451*, 293–296.
Hamersley, M. R., et al. (2007), Anaerobic ammonium oxidation in the Peruvian oxygen minimum zone, *Limnol. Oceanogr.*, *52*, 923–933.
Hou, L. J., Y. L. Zheng, M. Liu, J. Gong, X. L. Zhang, G. Y. Yin, and L. You (2013), Anaerobic ammonium oxidation (anammox) bacterial diversity, abundance, and activity in marsh sediments of the Yangtze Estuary, *J. Geophys. Res. Biogeosci.*, *118*, 1237–1246, doi:10.1002/jgrg.20108.
Hou, L. J., Y. L. Zheng, M. Liu, X. F. Li, X. B. Lin, G. Y. Yin, J. Gao, F. Y. Deng, F. Chen, and X. F. Jiang (2015), Anaerobic ammonium oxidation and its contribution to nitrogen removal in China's coastal wetlands, *Sci. Rep.*, *5*, 15,621, doi:10.1038/srep15621.
Hu, B., L. Shen, P. Du, P. Zheng, X. Xu, and J. Zeng (2012), The influence of intense chemical pollution on the community composition, diversity and abundance of anammox bacteria in the Jiaojiang Estuary (China), *PLoS One*, *7*, e33826.
Jensen, M. M., M. M. M. Kuyoers, G. Lavik, and B. Thamdrup (2008), Rates and regulation of anaerobic ammonium oxidation and denitrification in the Black Sea, *Limnol. Oceanogr.*, *53*, 23–36.
Jetten, M. S. M., H. J. M. Op den Camp, J. G. Kuenen, and M. Strous (2010), Description of the order Brocadiales, in *Bergey's Manual of Systematic Bacteriology*, vol. 4, edited by N. R. Krieg et al., pp. 506–603, Springer, Heidelberg, Germany.
Jickells, T. D. (1998), Nutrient biogeochemistry of the coastal zone, *Science*, *281*, 217–222.
Kartal, B., J. Rattray, L. A. van Niftrik, J. van de Vossenberg, M. C. Schmid, S. Schouten, J. A. Fuerst, J. S. Damsté, M. S. Jetten, and M. Strous (2007), *Candidatus 'Anammoxoglobus propionicus'* a new propionate oxidizing species of anaerobic ammonium oxidizing bacteria, *Syst. Appl. Microbiol.*, *30*, 39–49.
Kim, I. N., K. Lee, N. Gruber, D. M. Karl, J. L. Bullister, S. Yang, and T. W. Kim (2014), Increasing anthropogenic nitrogen in the North Pacific Ocean, *Science*, *346*, 1102–1106.
Koop-Jakobsen, K., and A. E. Giblin (2009), Anammox in tidal marsh sediments: The role of salinity, nitrogen loading, and marsh vegetation, *Estuaries Coasts*, *32*, 238–245.
Kuypers, M. M. M., A. O. Sliekers, G. Lavik, M. Schmid, B. B. Jorgensen, J. G. Kuenen, J. S. Sinninghe Damsté, M. Strous, and M. S. M. Jetten (2003), Anaerobic ammonium oxidation by anammox bacteria in the Black Sea, *Nature*, *422*, 608−611.
Li, M., Y. Hong, H. Cao, and J. D. Gu (2013), Community structures and distribution of anaerobic ammonium oxidizing and *nirS*-encoding nitrite-reducing bacteria in surface sediments of the South China Sea, *Microbiol. Ecol.*, *66*, 281–296.
Li, X. F., L. J. Hou, M. Liu, Y. L. Zheng, G. Y. Yin, X. B. Lin, L. Cheng, Y. Li, and X. T. Hu (2015), Evidence of nitrogen loss from anaerobic ammonium oxidation coupled with ferric iron reduction in an intertidal wetland, *Environ. Sci. Technol.*, *49*, 11,560–11,568.
Lozupone, C., M. E. Lladser, D. Knights, J. Stombaugh, and R. Knight (2011), UniFrac: An effective distance metric for microbial community comparison, *ISME J.*, *5*, 169–172.
Mohamed, N. M., K. Saito, Y. Tal, and R. T. Hill (2010), Diversity of aerobic and anaerobic ammonia-oxidizing bacteria in marine sponges, *ISME J.*, *4*, 38–48.
Mulder, A., A. A. Graaf, L. A. Robertson, and J. G. Kuenen (1995), Anaerobic ammonium oxidation discovered in a denitrifying fluidized bed reactor, *FEMS Microbiol. Ecol.*, *16*, 177−184.
Naeher, S., A. Huguet, C. L. Roose-Amsaleg, A. M. Laverman, C. Fosse, M. F. Lehmann, S. Derenne, and J. Zopfi (2015), Molecular and geochemical constraints on anaerobic ammonium oxidation (anammox) in a riparian zone of the Seine Estuary (France), *Biogeochemistry*, *123*, 237–250.
Papaspyrou, S., C. J. Smith, L. F. Dong, C. Whitby, A. J. Dumbrell, and D. B. Nedwell (2014), Nitrate reduction functional genes and nitrate reduction potentials persist in deeper estuarine sediments. Why?, *PLoS One*, *9* e94111.
Petersen, D. G., S. J. Blazewicz, M. Firestone, D. J. Herman, M. Turetsky, and M. Waldrop (2012), Abundance of microbial genes associated with nitrogen cycling as indices of biogeochemical process rates across a vegetation gradient in Alaska, *Environ. Microbiol.*, *14*, 993–1008.
Plummer, P., C. Tobias, and D. Cady (2015), Nitrogen reduction pathways in estuarine sediments: Influences of organic carbon and sulfide, *J. Geophys. Res. Biogeosci.*, *120*, 1958–1972, doi:10.1002/2015JG003057.
Quan, Z. X., S. K. Rhee, J. E. Zuo, Y. Yang, J. W. Bae, J. R. Park, S. T. Lee, and Y. H. Park (2008), Diversity of ammonium-oxidizing bacteria in a granular sludge anaerobic ammonium-oxidizing (anammox) reactor, *Environ. Microbiol.*, *10*, 3130–3139.
Rich, J. J., O. R. Dale, B. Song, and B. B. Ward (2008), Anaerobic ammonium oxidation (anammox) in ChesapeakeBay sediments, *Microbiol. Ecol.*, *55*, 311–320.
Risgaard-Petersen, N., R. L. Meyer, M. Schmidt, M. S. M. Jetten, A. E. Prast, S. Rysgaard, and N. P. Revsbech (2004), Anaerobic ammonia oxidation in an estuarine sediment, *Aquat. Microbial. Ecol.*, *36*, 293−304.
Roden, E. E., and D. R. Lovley (1993), Evaluation of ^{55}Fe as a tracer of Fe(III) reduction in aquatic sediments, *Geomicrobiol. J.*, *11*, 49–56.
Rysgaard, S., P. Thastum, T. Dalsgaard, P. Christensen, and N. Sloth (1999), Effects of salinity on NH_4^+ adsorption capacity, nitrification, and denitrification in Danish estuarine sediments, *Estuaries Coasts*, *22*, 21–30.
Schloss, P. D., et al. (2009), Introducing mothur: Open-source, platform-independent, community-supported software for describing and comparing microbial communities, *Appl. Environ. Microbiol.*, *75*, 7537–7541.
Schmid, M. C., U. Twachtmann, M. Klein, M. Strous, S. Juretschko, M. S. M. Jetten, J. Metzger, K. Schleifer, and M. Wagner (2000), Molecular evidence for genus level diversity of bacteria capable of catalyzing anaerobic ammonium oxidation, *Syst. Appl. Microbiol.*, *23*, 93–106.

Schmid, M. C., et al. (2005), Bio-markers for in situ detection of anaerobic ammonium-oxidizing (anammox) bacteria, *Appl. Environ. Microbiol.*, *71*, 1677–1684.
Schmid, M. C., et al. (2007), Anaerobic ammonium-oxidizing bacteria in marine environments: Widespread occurrence but low diversity, *Environ. Microbiol.*, *9*, 1476–1484.
Seitzinger, S. P. (2008), Nitrogen cycle: Out of reach, *Nature*, *452*, 162–163.
Shen, L. D., B. L. Hu, P. Zheng, Y. C. Qian, T. T. Chen, A. Hu, and L. P. Lou (2011), Molecular detection of anammox bacteria in the sediment of West Lake, Hangzhou, *Acta Sci. Circum.*, *31*, 1609–1615.
Strous, M., J. A. Fuerst, E. H. M. Kramer, S. Logemann, G. Muyzer, K. T. van de Pas-Schoonen, R. Webb, J. G. Kuenen, and M. S. M. Jetten (1999), Missing lithotroph identified as new planctomycete, *Nature*, *400*, 446–449.
Tamura, K., J. Dudley, M. Nei, and S. Kumar (2007), MEGA4: Molecular evolutionary genetics analysis (MEGA) software version 4.0, *Mol. Biol. Evol.*, *24*, 1596−1599.
Teixeira, C., C. Magalhães, S. B. Joye, and A. A. Bordalo (2014), The contribution of anaerobic ammonium oxidation to nitrogen loss in two temperate eutrophic estuaries, *Estuarine Coastal Shelf Sci.*, *143*, 41–47.
ter Braak, C. J. F., and P. Šmilauer (2002), CANOCO reference manual and CanoDraw for windows user's guide: Software for canonical community ordination (version 4.5) microcomputer power (Ithaca NY, USA).
Thamdrup, B., and T. Dalsgaard (2002), Production of N_2 through anaerobic ammonium oxidation coupled to nitrate reduction in marine sediments, *Appl. Environ. Microbiol.*, *68*, 1312–1318.
Thompson, J. D., T. J. Gibson, F. Plewniak, F. Jeanmougin, and D. G. Higgins (1997), The CLUSTAL_X windows interface: Flexible strategies for multiple sequence alignment aided by quality analysis tools, *Nucleic Acids Res.*, *25*, 4876−4882.
Trimmer, M., J. C. Nicholls, and B. Deflandre (2003), Anaerobic ammonium oxidation measured in sediments along the Thames Estuary, United Kingdom, *Appl. Environ. Microbiol.*, *69*, 6447−6454.
Trimmer, M., J. C. Nicholls, N. Morley, C. A. Davies, and J. Aldridge (2005), Biphasic behavior of anammox regulated by nitrite and nitrate in an estuarine sediment, *Appl. Environ. Microbiol.*, *71*, 1923–1930.
Wang, S., G. B. Zhu, Y. Z. Peng, M. S. M. Jetten, and C. Yin (2012), Anammox bacterial abundance, activity, and contribution in riparian sediments of the Pear River Estuary, *Environ. Sci. Technol.*, *46*, 8834–8842.
Wang, Y. F., and J. D. Gu (2014), Effects of allylthiourea, salinity, and pH on ammonia/ammonium-oxidizing prokaryotes in mangrove sediment incubated in laboratory microcosms, *Appl. Microbiol. Biotechnol.*, *98*, 3257–3274.
Yang, Y. P., Y. T. Li, Z. H. Sun, and Y. Y. Fan (2014), Suspended sediment load in the turbidity maximum zone at the Yangtze River Estuary: The trends and causes, *J. Geogr. Sci.*, *24*, 129–142.
Yang, Y. P., M. J. Zhang, Y. T. Li, and W. Zhang (2015), The variations of suspended sediment concentration in Yangtze River Estuary, *J. Hydrodyn.*, *27*, 845–856.
Yin, G. Y., L. J. Hou, M. Liu, Z. F. Liu, and W. S. Gardner (2014), A novel membrane inlet mass spectrometer method to measure $^{15}NH_4^+$ for isotope-enrichment experiments in aquatic ecosystems, *Environ. Sci. Technol.*, *48*, 9555–9562.
Yoshinaga, I., T. Amano, T. Yamagishi, K. Okada, S. Ueda, and Y. Sako (2011), Distribution and diversity of anaerobic ammonium oxidation (anammox) bacteria in the sediment of a eutrophic freshwater lake, Lake Kitaura, Japan, *Micorbes Environ.*, *26*, 189–197.
Yuan, R., H. Wu, J. R. Zhu, and L. Li (2016), The response time of the Changjiang plume to river discharge in summer, *J. Mar. Syst.*, *154*, 82–92.
Zhang, Y., X. Ruan, H. J. M. Op den Camp, T. J. M. Smits, M. S. M. Jetten, and M. C. Schmid (2007), Diversity and abundance of aerobic and anaerobic ammonium-oxidizing bacteria in freshwater sediments of the Xinyi River (China), *Environ. Microbiol.*, *9*, 2375–2382.
Zheng, Y. L., et al. (2016), Tidal pumping facilitates dissimilatory nitrate reduction in intertidal marshes, *Sci. Rep.*, *6*, 21,338.